Journal of NUCLEAR SCIENCE and TECHNOLOGY, Supplement 4, p. 361–364 (March 2004)

Study of Radiation Hardness of Silicon Pixel Detectors after Neutron and Proton Irradiations

Hyosung CHO[1,*], Sanghyo HAN[2], Sanghee NAM[3], Chihyung CHIEN[4]

[1]*Department of Radiation Science, Institute of Health Science, Research Institute of Medical Engineering Basic Atomic Energy Research Institute, Yonsei University, Wonju 220-710, Korea*
[2]*PEFP, Korea Atomic Energy Research Institute, Daejon 305-600, Korea*
[3]*Medical Imaging Research Center, Inje University, Kimhae 621-749, Korea*
[4]*Department of Physics, Johns Hopkins University, Baltimore, MD 21218, USA*

A new design of silicon pixel detectors with $n^+/n/p^+$ (pixel array/bulk/pad) configuration has been developed for more radiation-tolerant CMS forward pixel sensors. In this design, a single (640 μm wide) n^+ implant is placed on the n^+ side, and guard rings on the p^+ side are always kept active before and after type inversion. The whole n^+ side is grounded and connected to readout chips. All tested devices were fabricated from both standard (normal) and oxygen-enriched silicon wafers, and radiation-hardness effects after neutron (1 MeV equivalent) and proton (24 GeV) irradiations of these devices were investigated. Other electrical characteristics such as the leakage current and the potential distribution over guard rings were tested using standard measurement techniques.

KEYWORDS: Silicon pixel detector, radiation damage, radiation hardness, guard ring, CMS experiment

I. Introduction

The lifetime of silicon detectors in a severe radiation environment depends strongly upon careful detector design and material selection due to the anticipated radiation-induced damage. This damage effect includes an increase of leakage current, a change of effective dopant concentration (N_{eff}), resulting in type inversion and unlimited growth of full depletion voltage (V_{fd}), and a decrease in charge collection efficiency, mainly due to the significant creation of radiation defects in detector material [1]. There are several technical approaches to enhance the radiation hardness of silicon pixel detectors [2,3]. Our approach to this problem started with detectors of $n^+/n/p^+$ and double-sided guard ring configurations. Here the $n^+/n/p^+$ configuration was chosen to allow detectors to operate even in partial depletion mode after type inversion and thus at a reasonably low bias voltage, and the double-sided guard ring configuration to reduce electric field concentration near the junction boundary and also to provide an electrical sink for leakage current generated outside the device active area. **Figure 1** shows a schematic diagram of our pixel design, referred to as GR_10 design. In this design, a single (640 μm wide) n^+ implant is placed on the n^+ side, and guard rings on the p^+ side are always kept active before and after type inversion. The whole n^+ side is grounded and connected to readout chips, which greatly simplifies detector assembling and improves the stability of bump-bonded readout chips. Another technique to improve radiation hardness of silicon detectors is to dope oxygen impurities into silicon wafers. The doped oxygen impurities may reduce the formation of main defect complexes (i.e., double vacancy) by capturing radiation-created vacancies by the oxygen impurities [4,5].

*Corresponding author, Tel.+82-33-760-2428, Fax.+82-33-760-2815, E-mail; hscho@dragon.yonsei.ac.kr

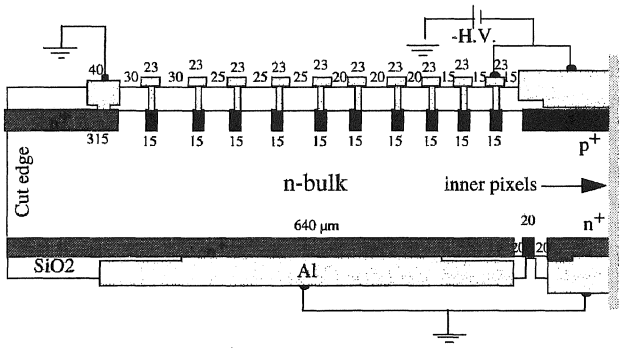

Fig. 1 A schematic diagram of our new pixel design (GR_10). For brevity inner pixel area is not shown in this figure.

In this study, we used a new pixel detector which had been fabricated from both standard (normal) and oxygen-enriched silicon wafers, and the radiation-hardness effects after neutron (1 MeV equivalent) and proton (24 GeV) irradiations of these devices were investigated to fabricate better radiation-hardened silicon pixel detectors for the CMS experiment. Other electrical characteristics such as the leakage currents and the potential distribution over the guard rings were tested, using the standard techniques of I-V, V-V, and transient current technique (TCT) before and after the irradiations.

II. Results and Discussion

1. Wafers and Irradiation

All tested devices were fabricated from two different silicon wafers: (a) a standard (normal) float-zone (FZ) n-type silicon wafer with a thickness of 280 μm and a resistivity of 1.2 kΩ·cm, oxidized at 1100 ℃ for 6 hours in

oxygen atmosphere, and (b) an oxygen-enriched wafer with a thickness of 400 μm and a resistivity of 4.4 kΩ·cm, also oxidized at 1200 ℃ for 9 days to obtain high and uniform oxygen concentration over the whole wafer thickness. Oxygen concentrations measured in the bulk were about $1.5x10^{16}$ O/cm^3 for the standard wafer and about $3.9x10^{17}$ O/cm^3 for the oxygen-enriched wafer. Electrical properties of both wafers are summarized in **Table 1**.

Table 1 Electrical properties of standard and oxygen-enriched silicon wafers.

Properties / Wafers	Detector thickness	Resistivity	Oxide thickness	Oxygen density in bulk
Standard (#928)	280 μm	1.2 kΩcm	0.5 μm	~$1.5x10^{16}$ (O/cm^3)
Oxygen—enriched (#933)	400 μm	4.4 kΩcm	3.0 μm	~$3.9x10^{17}$ (O/cm^3)

For radiation-hardness comparison of these detectors, we used two radiation sources: (a) neutron (1 MeV equivalent) up to $3.7x10^{14}$ n/cm^2 at the University of Massachusetts Lowell, and (b) proton (24 GeV) up to $4.9x10^{14}$ p/cm^2 in the Proton Synchrotron (PS) accelerator at CERN. All measurements before and after irradiation were made at room temperature with a microprobe station. The detectors had been kept −15℃ to slow down reverse-annealing process.

2. Full Depletion Voltage (V_{fd})

In order to compare radiation hardness between the standard and the oxygen-enriched detectors, we measured full depletion voltages (V_{fd}) of the detectors, using the TCT. **Figure 2** shows a block diagram of the TCT setup. Here a pulse generator (Hewlett Packard 8111A) transforms nanosecond pulses into current pulses for laser pumping. A laser light with a wave length of 670 nm and 1 nsec width is injected to detectors mounted on a sample holder from the front or the back side to generate free charge carriers close to detector surface (about 15 μm). A digital oscilloscope (TDS-744), directly connected to a coupling capacitor (2000 pF), was used to measure TCT output signal through a 50 Ω input impedance. More details of the TCT measurement setup is described elsewhere [6].

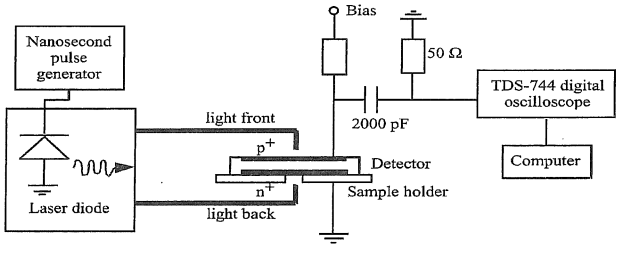

Fig. 2 A block diagram of the TCT setup which consists of a pulse generator, a laser diode, and an oscilloscope.

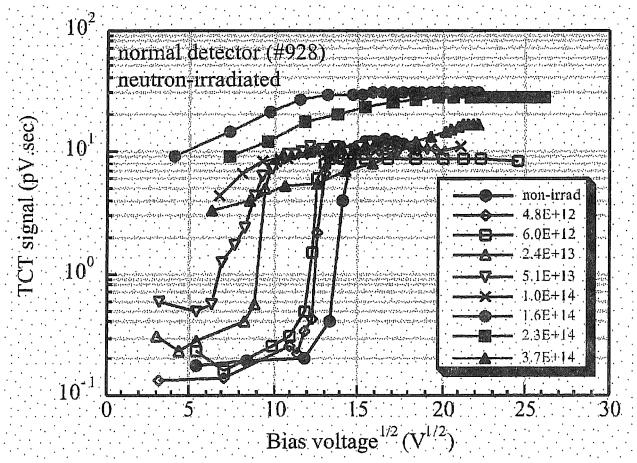

Fig. 3 An example of TCT measurements using the standard (normal) detectors before and after irradiation to various neutron fluences up to $3.7x10^{14}$ n/cm^2.

Figure 3 shows an example of TCT measurements using the standard detectors before and after irradiation to various neutron fluences. The laser light was always injected to the low field side (i.e., the n^+ side before type inversion and the p^+ side after type inversion) for more accurate determination of full depletion voltage. It was taken as the voltage at which the TCT signal reaches a certain saturation point. In **Fig. 3**, the difference in the saturation values for the front and back side injection of the laser light is probably due to different opening area on each side for laser light transmission. **Figures 4** and **5** show variations of the full depletion voltage after neutron and proton irradiations, respectively. Since the thicknesses of the detectors are different, we normalized the full depletion voltages to a thickness of 280 μm for comparison. From these measurements we compared the radiation-hardness effects for neutrons and protons of standard and oxygen-enriched detectors in terms of the rate at which the full depletion voltage increases after type inversion. The difference in type inversion points for those detectors is due to their different pre-irradiated resistivities.

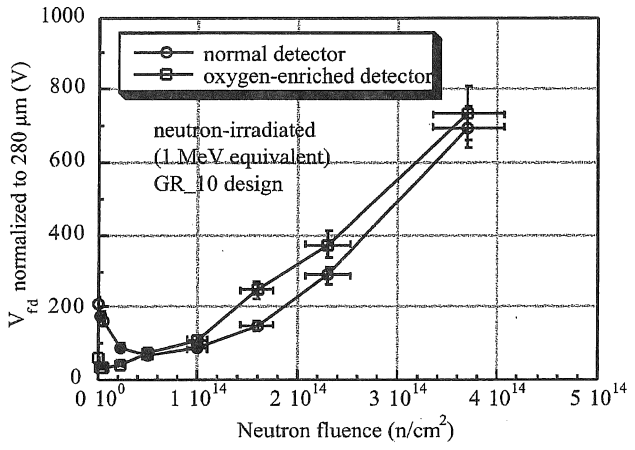

Fig. 4 Variations of the full depletion voltages with 1 MeV equivalent neutron-irradiation fluences.

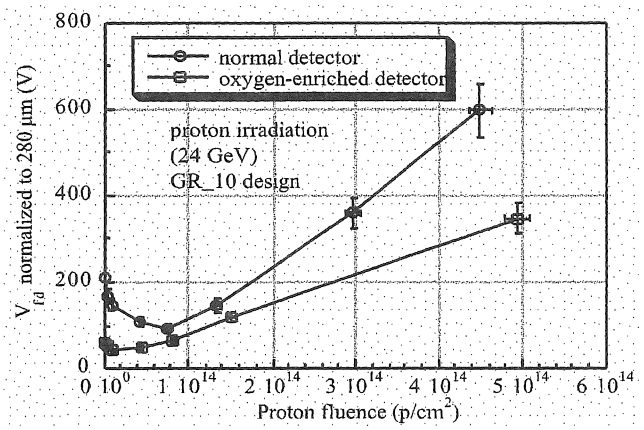

Fig. 5 Variations of the full depletion voltages as a function of 24 GeV proton irradiation fluences.

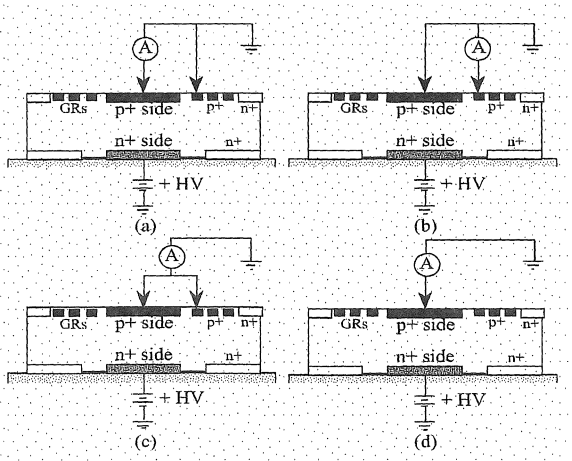

Fig. 7 Four different electrical circuits used for leakage current measurements in **Fig. 6.**

As shown in **Figs. 4** and **5**, the behavior of the full depletion voltage was much different between the standard and oxygen-enriched detectors, and oxygen impurities doped to silicon substrates sensitively depended on the kind of irradiating particles. For proton irradiation, the increase rate of the full depletion voltage after type inversion was higher by a factor of about two for the standard detector than for the oxygen-enriched detector (**Fig. 5**), but no noticeable difference was observed for neutron irradiation (**Fig. 4**).

3. Leakage Current

Figure 6 shows the leakage currents measured for the standard detector before irradiation. Here the n^+ side was positively biased up to 500 V, and the leakage current was measured from the p^+ contact and/or the innermost guard ring, using four different electrical circuits, shown in **Fig. 7**. The bulk leakage current was measured using the circuit (a). It was very small in the range of 10^{-4} – 10^{-3} μA up to 260 V, and it is mainly caused by the thermal generation of charge carriers in bulk, and then increased continuously. The

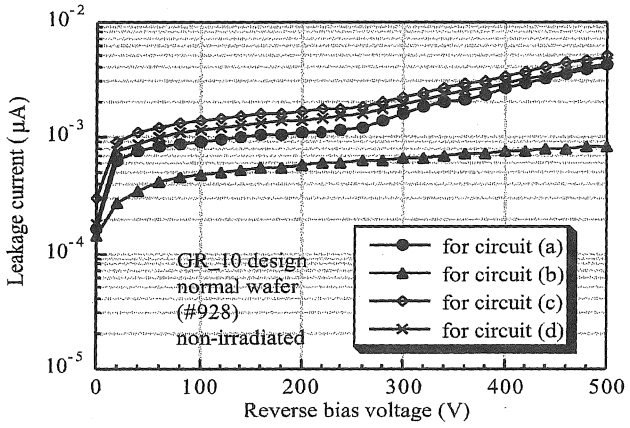

Fig. 6 Leakage current measurements before irradiation, using the standard detector. Here the leakage current was measured using four different circuits in **Fig. 7.**

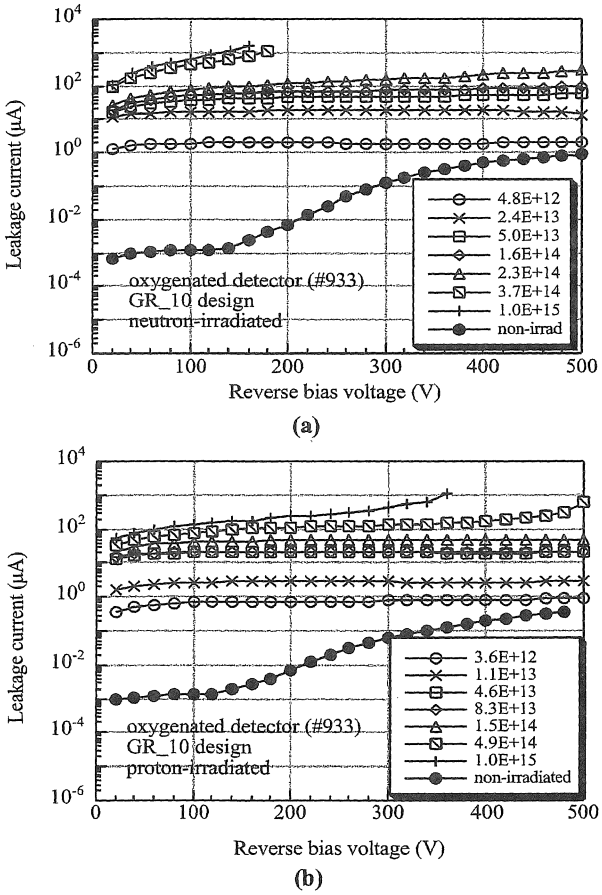

Fig. 8 Leakage current measurement after **(a)** neutron and **(b)** proton irradiations, using the oxygen-enriched detectors.

surface leakage current was measured using the circuit (b), and was about half the size of the bulk leakage current at a bias voltage of 200 V. Total leakage current from the bulk and surface was measured using two different circuits of (c) and (d). In this paper all other measurements of leakage currents were performed using the circuit (a). **Figure 8** shows examples of the leakage currents measured for the oxygen-enriched detectors before and after irradiation to

various (a) neutron and (b) proton fluences. The leakage current before irradiation was very small (about 10^{-3} μA) before full depletion but increased continuously over a bias voltage of 160 V. However, after irradiation it increased significantly with fluence, more than 5 orders of magnitude at the full design fluences, but no breakdown was observed up to a bias voltage of 500 V. Note, however, that these measurements were performed at room temperature without cooling, and the problems associated with the large leakage current will be minimized by operation at reduced temperature (e.g., - 15℃ in the CMS experiment).

4. Potential Distribution over the Guard Rings

Figure 9 shows the potential distribution over the guard rings **(a)** before and **(b)** after irradiation at a neutron fluence of $2.3x10^{14}$ n/cm^2 using the oxygen-enriched detectors. In these measurements the n^+ side and the edge region of the p^+ side were grounded, while the p^+ contact and the innermost guard ring negatively biased up to 200 V. As shown in **Fig. 9 (a)**, before irradiation some of outside guard rings are not yet activated up to 200 V, indicating that the lateral expansion of the depletion junction has not yet reached those guard rings even when the detector become fully depleted. After irradiation, however, all of the guard rings are activated at 200 V by punch through, and the bias voltage are more evenly distributed over the guard rings. There was no more potential drop on the n^+ side and across device edge, giving advantages for safe operation of the detectors at a high biasing voltage and for stability of readout chips.

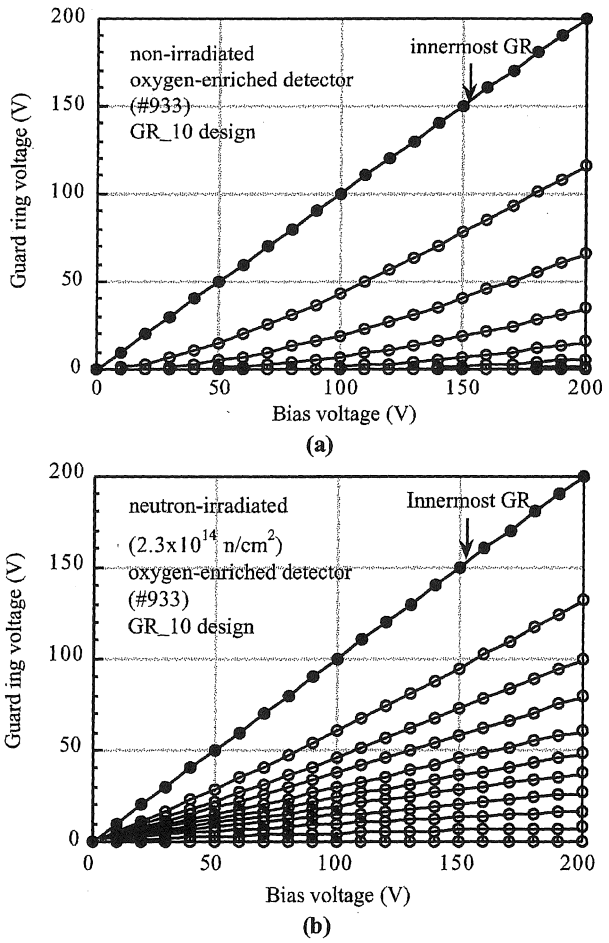

Fig. 9 Potential distribution over guard rings (a) before and (b) after neutron irradiation at a fluence of $2.3x10^{14}$ n/cm^2.

III. Conclusion

A new design of silicon pixel detectors has been developed for more radiation-tolerant CMS forward pixel sensors. In this design, a single (640 μm wide) n^+ implant is placed on the n^+ side, and guard rings on the p^+ side are always kept active before and after type inversion. The whole n^+ side is grounded and connected to readout chips. The leakage currents of all devices were very small (~10^{-3} μA) before irradiation, but after irradiation significantly increased (more than 5 orders of magnitude at the full design fluence). The bias potential distributes evenly over the guard rings after type inversion, and no breakdown was observed up to a bias voltage of 500 V. The behavior of the full depletion voltage with particle fluence was much different between standard and oxygen-enriched detectors, and the effect of oxygen impurities doped to silicon substrate was sensitive to the type of irradiation. Oxygen-enriched detectors have better radiation hardness (by a factor of two) than standard detectors with proton irradiation, but no noticeable difference was observed with neutron irradiation.

Acknowledgement

This work was supported by the RRC program of MOST and KOSEF for 2003.

References

1) W. Chen, V. Eremin, Z. Li, et al., "Design and processing of various configurations of silicon pixel detectors for high irradiation tolerance up to 6x1014 n/cm^2 in LHC application," *IEEE Trans. on Nuclear Science*, **45(3)**, 348 (1998).
2) D. Menichelli, M. Bruzzi, Z. Li, V. Eremin, "Modeling of observed double-junction effect," *Nucl. Instrum. Methods*, **A426**, 135 (1999).
3) H.S. Cho, X.B. Xie, et al., "Characterization of silicon pixel detector with $n^+/n/p^+$ and double-sided multiguard ring structure before and after neutron irradaition," *IEEE Trans. on Nuclear Science*, **47(3)**, 772 (2000).
4) Z. Li, W. Chen, L. Dou, et al., "Investigation of the oxygen-vacancy (A-center) defect complex profile in neutron irradiated high resistivity silicon junction particle detectors," *IEEE Trans. on Nuclear Science*, **42(4)**, 219 (1995).
5) Z. Li, H.W. Kraner, et al., "Study of the long term stability of the effective concentration of ionized space charge (N_{eff}) of neutron irradiated silicon detectors fabricated by various thermal oxidation processes," *IEEE Trans. on Nuclear Science*, **39(6)**, 1730 (1992).
6) V. Eremin, et al., "Development of transient current and charge techniques for the measurement of effective net concentration of ionized charges (N_{eff}) in the space charge region of p-n junction detectors," *Nucl. Instrum. Methods*, **A372**, 388 (1996).